Fish and Shellfish Immunology 92 (2019) 141–150

Contents lists available at ScienceDirect

Fish and Shellfish Immunology

journal homepage: www.elsevier.com/locate/fsi

Full length article

Identification and functional analysis of the Mandarin fish (*Siniperca chuatsi*) hypoxia-inducible factor-1α involved in the immune response

Jian He[a,1], Yang Yu[a,1], Xiao-Wei Qin[b], Ruo-Yun Zeng[b], Yuan-Yuan Wang[a], Zhi-Min Li[a], Shu Mi[a], Shao-Ping Weng[b], Chang-Jun Guo[a,b,c,*], Jian-Guo He[a,b,c]

[a] State Key Laboratory for Biocontrol / Guangdong Provincial Key Laboratory of Marine Resources and Coastal Engineering, School of Marine Sciences, Sun Yat-sen University, No.132 Waihuan Dong Road, Higher Education Mega Center, Guangzhou, Guangdong, 510006, PR China
[b] Southern Marine Science and Engineering Guangdong Laboratory (Zhuhai), Zhuhai, 519000, China
[c] Institute of Aquatic Economic Animals / Guangdong Province Key Laboratory for Aquatic Economic Animals, School of Life Sciences, Sun Yat-sen University, 135 Xingang Road West, Guangzhou, 510275, PR China

ARTICLE INFO

Keywords:
Hypoxia
HIF-1α
Immune response
Mandarin fish

ABSTRACT

Mandarin fish (*Siniperca chuatsi*) is a popular cultured freshwater fish species due to its high market value in China. With increasing density of breeding, mandarin fish is often cultured under low environmental oxygen concentrations (hypoxia). In this study, the relative expression levels of hypoxia response element (HRE)-luciferase reporter and the HIF signaling pathway downstream genes (*scldha*, *scvegf*, and *scglut-1*) were significantly increased by hypoxic stress, thereby indicating that mandarin fish has an HIF signaling pathway. The mandarin fish HIF-1α (*sc*HIF-1α) was also characterized. Multiple sequence alignments showed that *sc*HIF-1α presented similar architectures to other known vertebrates. Subcellular localization analysis showed that *sc*HIF-1α was mainly located in the nucleus of the mandarin fish fry-1 (MFF-1) cells. The role of *sc*HIF-1α in the regulation of the HIF signaling pathway was confirmed. Overexpression of *sc*HIF-1α could induce the HIF signaling pathway, whereas knockdown of *sc*HIF-1α inhibited the activity of the HIF-1 signaling pathway. Tissue distribution analysis showed that *schif-1α* was significantly highly expressed in the blood, heart, and liver, which indicated that the main function of *sc*HIF-1α was closely related to the circulatory system. Furthermore, *sc*HIF-1α expression was significantly induced by poly I:C, poly dG:dC or PMA, thereby indicating that *sc*HIF-1α was involved in the immune response. HIF-1α plays an important role in pathogen infections in mammals, but its role in fish is rarely investigated. Overexpression of *sc*HIF-1α could inhibit MRV and SCRV infections, whereas knockdown of *sc*HIF-1α could promote such infections. Those results suggested that *sc*HIF-1α played an important role in fish virus infection. Our study will help understand the hypoxia associated with the outbreaks of aquatic viral disease.

1. Introduction

The hypoxia-inducible factor (HIF) signaling pathway is an important intracellular metabolism regulation pathway that maintains the stability of tissues and cells in a hypoxic environment [1]. HIF-1 is a key protein in the HIF signaling pathway [2]. HIF-1 can combine with HIF-reactive elements (HREs) in the DNA sequence and recruit the p300/CBP protein to initiate the downstream gene transcription of the components involved in glucose metabolism and angiogenesis; these components include vascular endothelial growth factor (VEGF), glucose transporter 1/-3 (Gult1/3), hexokinase 2 (HK2), and lactate dehydrogenase A (LDHA) [3]. Moreover, HIF-1 is a heterodimer that is mainly composed of two subunits (HIF-1α and HIF-1β): the HIF-1α subunit is an O_2-regulated protein, and the HIF-1β subunit is stably expressed in the cytoplasm [4]. The HIF-1α subunit is degraded by the ubiquitin proteolytic complex, and the activation of the HIF signaling pathway is inhibited under normal oxygen saturation [5,6]. In hypoxia, the degradation of HIF-1α is inhibited and its protein level increases rapidly; HIF-1α binds to HIF-1β and regulates the expression of many genes to enable cells to adapt in hypoxia [7]. Fishes also have a HIF pathway and possess homologs of HIF-α. The fish HIF-1α sequence was first reported by using rainbow trout. To date, HIF-1α sequences have

* Corresponding author. State Key Laboratory for Biocontrol / Guangdong Provincial Key Laboratory of Marine Resources and Coastal Engineering, School of Marine Sciences, Sun Yat-sen University, No.132 Waihuan Dong Road, Higher Education Mega Center, Guangzhou, Guangdong, 510006, PR China..
E-mail address: gchangj@mail.sysu.edu.cn (C.-J. Guo).
[1] These authors contributed equally to this work.

https://doi.org/10.1016/j.fsi.2019.04.298
Received 16 January 2019; Received in revised form 24 April 2019; Accepted 27 April 2019
Available online 05 June 2019
1050-4648/

Table 1
Primers used for cDNA cloning of *sc*HIF-1α conserved regions.

Name (For initial PCR)	Sequence (5′–3′)
5′ RACE for *sc*HIF-1α-F	CTAATAGCACTCACTATAGGGCAAGCAGTGGTATCAACGCAGAGT
5′ RACE for *sc*HIF-1α-R	CCAGAGACAAGATCACTTTCTCCTC
3′ RACE for *sc*HIF-1α-F	GATCTATCTCTCCGAGAATGTCAAC
3′ RACE for *sc*HIF-1α-R	ACTCTGCGTTGATACCACTGCTTGCCCTATAGTGAGTGCTATTAG
*sc*HIF-1α-F1	ATGGACACAGGAATTGTACCAGAAAAG
*sc*HIF-1α-R1	TCAGTTGACGTGGTCCAGAGC

been reported in several fish species, e.g., in the Atlantic croaker (*Micropogonias undulatus*), zebrafish (*Danio rerio*), and perch (*Perca fluviatilis*) [8].

Increasing evidence demonstrates that hypoxia also regulates many innate immunological functions, including cell migration; apoptosis; the phagocytosis of pathogens; antigen presentation; and the production of cytokines, chemokines, and angiogenic and antimicrobial factors [9]. On the one hand, many immune-related genes are regulated by HIF-1, either directly via the binding of HIF to a HRE in the promoter region, or indirectly via the HIF-mediated induction of other signaling molecules and transcription factors [9]. For instance, the *ifng* promoter contains a functional HRE and hypoxic induction of IFNγ; HIF-1 also binds to a highly polymorphic region of the promoter encoding solute carrier family member 1 (Slc11a1), a phagocyte-specific solute carrier that induces the expression of cytokines, chemokines, and MHC class II molecules [10]. Moreover, CCL5 and C-X-C motif chemokine 12 (CXCL12, also known as SDF1a) production is driven by HIF-1α [11,12]. On the other hand, the HIF signaling pathway is regulated by the immune system. For example, nuclear factor-κB (NF-κB), which plays a central role in regulating the immune response to infection, is also required for the bacteria-induced HIF-1α mRNA transcriptional response in macrophages [13]. Furthermore, T cell receptor (TCR) ligation induces the substantial accumulation of HIF-1α mRNA and protein by a mechanism dependent on STAT3 [14–16]. Finally, tumor necrosis factor-α (TNF-α), another key host inflammatory mediator, can induce HIF-1α expression in macrophages [17].

Viral infection of a host rapidly triggers intracellular signaling events. The HIF signaling pathway also plays an important role in pathogenic infections [18]. Hypoxia usually induces to restrict the replication of viruses, such as the reduction in adenoviral production and cytolytic activity under hypoxic conditions; moreover, the replication of vesicular stomatitis virus is inhibited by hypoxia-induced HIF-1α [19]. Conversely, some viruses can reprogram cell bioenergetics toward lowering cellular respiration, such as HIV-1 Vpr forming a heterodimer with HIF-1α to stimulate HIV-1 gene transcription and the promoter of the John Cunningham virus being bound and activated by HIF-1α [20,21]. With increasing density of breeding, fishes are often cultured under low environmental oxygen concentrations (hypoxia). In recent years, the influence of hypoxia on outbreaks of aquatic viral disease has attracted considerable research attention. However, the role of HIF-1α in viral infections in fish is rarely investigated.

The mandarin fish *Siniperca chuatsi*, which belongs to Serranidae in the order Perciformes, is a popular cultured freshwater fish species due to its high market value in China. At present, the mandarin fish HIF pathway remains unclear. To further clarify the influence of hypoxic stress on mandarin fish and its HIF signaling pathway, the functions of mandarin fish HIF-1α (*sc*HIF-1α) should be identified. In this study, the mandarin fish (*S. chuatsi*) HIF-1 pathway and *sc*HIF-1α were characterized. The mechanism by which *sc*HIF-1α regulates the HIF-1 signaling pathway was investigated. Furthermore, changes in the expression level of HIF-1α when encountering immunity stimulation was studied, and the role of HIF-1α in fish viral infection was preliminarily revealed.

2. Materials and methods

2.1. Cells and virus

The mandarin fish fry (MFF-1) cell line was constructed in our laboratory, cultured in Dulbecco's modified Engle's medium (DMEM; Gibco, USA), and supplemented with 10% fetal bovine serum (FBS; Gibco, USA) at 27 °C under humidified atmosphere containing 5% CO_2 [22]. The hypoxic cell culture system (BioSpherix, incubator subchamber proOx C21) to maintain the 1% oxygen content. The mandarin fish ranavirus (MRV) and *Siniperca chuatsi* rhabdovirus (SCRV) strains were separated from the diseased mandarin fish in 2017 and stored in our laboratory. MFF-1 cells for infection were cultured overnight in 25 cm^2 flasks at 5×10^6 cells prior to further treatment. Each flask was inoculated with the virus suspension (multiplicity of infection [MOI] = 1). The cells were harvested at different times following the experimental design. Viral titers were calculated according to the Reed–Muench and Spearman–Karber methods.

2.2. Cloning of Mandarin fish HIF-1α cDNA

To amplify the full-length of the *sc*HIF-1α gene, we performed PCR using the primers listed in Table 1. Total RNAs were extracted from MFF-1 cells using Trizol reagent (Invitrogen, USA) in accordance with the manufacturer's protocol and then treated with RNase-free DNase (Promega, USA) to remove the contaminating DNA. cDNAs were synthesized from 1 μg of total RNAs with murine leukemia virus reverse transcriptase (MLVRTase; Promega, USA) following the manufacturer's instruction and by using an Oligo(dT) 18 primer. cDNAs from MFF-1 cells were used as templates for PCR reactions. All PCR reactions were performed using the following conditions: 1 cycle of denaturation at 94 °C for 5 min; 30 cycles of 94 °C for 30 s, 55 °C for 30 s, and 72 °C for 2 min; and a 10 min extension at 72 °C. Finally, the PCR products were purified, cloned into the pMD18-T vector (Takara, Japan), and sequenced (Thermo Fisher Scientific, USA).

2.3. Sequence analysis

Homology sequences were obtained using the BLAST program at the National Center for Biotechnology Information (http://www.ncbi.nlm.nih.gov/blast). The deduced amino acid sequence of *sc*HIF-1α was analyzed using the Simple Modular Architecture Research Tool (SMART) program (http://smart.emblheidelberg.de/). Sequence alignment was performed using the Cluster X v1.83 program and edited with Gene Doc v2.6.002 software (http://www.nrbsc.org/gfx/genedoc/index.html). The phylogenetic tree was constructed using the Bootstrap N-J method of Molecular Evolutionary Genetics Analysis (MEGA) software version 5.0 program. Bootstrap sampling was reiterated 1000 times.

2.4. Dual luciferase reporter assays

MFF-1 cells were cultured in 24-well plates for 24 h before transfection. The hypoxia response element (HRE)-luciferase reporter plasmid (pGL4-HREs-luc, 0.4 μg), tested plasmid (0.4 μg), and pRL-TK

Table 2
Primers used for real-time quantitative RT-PCR.

Genes	Primers	Sequences (5′–3′)
schif-1α	Forward	CTCTGGAAGGCTTTCTCATGGTG
	Reverse	GGTCACAGGGATGTATGAAGTCAA
vegf	Forward	ACCGAAGGAAACAGAAAGAGG
	Reverse	CAGGACGGGATGAAGATGTG
ldha	Forward	GGTCTTCCTGAGCATCCCTT
	Reverse	TTCTCCTCTTCGGGCTTCA
glut 1	Forward	GGTTTATTGTGGCAGAGTTGTT
	Reverse	CCCACTATGAAGTTGGCAGTC
β-actin	Forward	CCCTCTGAACCCCAAAGCCA
	Reverse	CAGCCTGGATGGCAACGTACA

(40 ng) plasmid were co-transfected into the MFF-1 cells. The pRL-TK plasmid was transfected as an internal control. After 2 h, the transfection mixture was replaced with 500 μL of DMEM. Following 48 h of transfection, the total cell lysates were analyzed with the Dual Luciferase Reporter Gene Assay Kit (Promega) in accordance with the manufacturer's instructions. Luciferase activities were measured using Glomax (Promega). All experimentations involved at least three independent experiments with three technical replicates for each experiment.

2.5. Real-time quantitative RT-PCR

Real-time quantitative RT-PCR was performed with SYBR premix Ex Taq™ (Takara, Japan) on a LightCycler 480 instrument (Roche Diagnostics, Switzerland). The primers for quantitative PCR were designed using Primer Express software (Applied Biosystems; Table 2). For tissue-specific expression analysis, total RNAs from different tissues were prepared as previously described and reverse-transcribed using Takara's ExScript reverse transcription (RT) reagent kit (Takara, Japan) following the manufacturer's protocol. The expression levels of *schif-1α* and the HIF signaling pathway downstream genes (*scvegf*, *scglut1*, and *scldha*) were detected using the corresponding real-time forward and reverse primers (Table 2). All real-time PCR reactions were performed in triplicate. PCRs were performed on a total reaction volume of 10 μL containing 0.2 μM primers, 1 μL of cDNA, 5 μL of 2 × SYBR premix ExTaq™, and 3.6 μL of ultrapure water using the following setting: 40 cycles of amplification for 5 s at 95 °C, 40 s at 60 °C, and 1 s at 70 °C. The expression level of each transcript was normalized to the expression of the *β-actin* gene, which was used as an internal housekeeping control. The real-time quantitative PCR data of the target genes were analyzed using the Q-gene statistics add-in, followed by unpaired sample *t*-test. Statistical significance was accepted at $p < 0.05$, and high significance was accepted at $p < 0.01$. All data were expressed as the mean ± standard deviation (SD).

2.6. Cell transfection

Following standard methods, transient transfection of plasmids was conducted with Lipofectamine 2000 (Thermo Fisher Scientific, USA) in accordance with the manufacturer's instructions. Prior to transfection, MFF-1 cells were directly seeded in 24-well cell culture plates for subcellular localization analysis or luciferase reporter assays. Cells were transfected using Lipofectamine 2000 in serum-free culture medium (Opti-MEM, Gibco). After 2–4 h, the mixture was replaced with DMEM supplemented with 10% FBS. For siRNA transfection, the HiPerFect Transfection Reagent (Qiagen, USA) was used. Prior to transfection, the MFF-1 cells were directly seeded in 6-well cell culture plates with 2 mL of an appropriate culture medium containing FBS and antibiotics. Approximately 3 μL of HiPerFect Transfection Reagent was added to the diluted si-*sc*h-HIF-1a (5′ CCAGTCAAATCCCTTCAGA 3′), and both were mixed by vortexing. The control siRNA (siRNA-NC) was obtained from Guangzhou Ribobio Co., Ltd. The samples were incubated for 5–10 min at room temperature (approximately 25 °C) to allow for the formation of transfection complexes. Subsequently, the complexes were added dropwise onto the cells. The plate was gently swirled to ensure uniform distribution of the transfection complexes. The cells were incubated with the transfection complexes under normal growth conditions, and gene silencing was monitored after an appropriate time (e.g., 6–72 h after transfection, depending on the experimental setup). The medium was changed as required.

2.7. Antibodies and reagents

Antibodies specific for myc-tag were obtained from Sigma-Aldrich (USA). Alexa Fluor 594-labeled goat anti-rabbit IgG and Hoechst 33342 were obtained from Thermo Fisher Scientific (USA). The chemicals, poly I:C, poly dG:dC, and phorbol 12-myristate 13-acetate (PMA) used in this study were purchased from Sigma-Aldrich (USA).

2.8. Indirect immunofluorescence assay

The MFF-1 cell line was cultured in DMEM supplemented with 10% FBS at 27 °C under a humidified atmosphere containing 21% O_2 and 5% CO_2. The Endo-free pCMV-Myc-*sc*HIF-1α plasmid was transfected into MFF-1 cells using Lipofectamine 2000. At 48 h post-transfection, the MFF-1 cells were washed with sterile PBS buffer (pH 7.4) for 5 min, fixed with 3.7% paraformaldehyde, permeabilized with 0.5% Triton X-100, blocked for 1 h with 5% normal goat serum in PBS, and labeled with the primary antibodies. Antibody binding was detected using the secondary antibody conjugated with Alexa Fluor 594 (Thermo Fisher Scientific, USA). Hoechst 33342 (Thermo Fisher Scientific, USA) was used to counterstain the cell nuclei. The samples were examined under a confocal microscope (Zeiss LSM510, Germany).

2.9. Western blot analysis

The protein samples were mixed with 5 × loading buffer (250 mM Tris-HCl pH 6.8, 10% SDS, 5% β-mercaptoethanol, 50% glycerinum, and 0.5% bromophenol blue), boiled for 10 min, and subjected to SDS-PAGE for separation. The proteins were subsequently transferred onto nitrocellulose membranes (Amersham Biosciences). The nitrocellulose membranes were blocked in blocking buffer [5% (w/v) skim milk resolved in TBST buffer (20 mM Tris-HCl, 150 mM NaCl, 0.1% Tween 20, and pH 7.6)] at room temperature for 1 h. The membranes were washed three times for 10 min each with TBST. After being blocked, the membranes were incubated with the mouse anti-Myc antibody (Sigma-Aldrich, Germany) at room temperature for 2 h. The membranes were then washed three times for 10 min each with TBST. Conversely, some membranes were incubated with goat anti-Mouse IgG HRP Conjugate (Promega, USA) at room temperature for 1 h. The membranes were then washed three times for 10 min each with TBST. Protein bands were visualized using a high-sig chemiluminescence WB substrate kit (Tanon, China).

3. Results

3.1. Molecular characteristics of scHIF-1α

The cDNA fragment of *sc*HIF-1α was obtained from the transcriptome data (unpublished). To clone the full-length cDNA of *sc*HIF-1α, the 5′ and 3′ rapid-amplification of cDNA ends (RACE) reactions were performed using gene-specific primers (Table 1) designed from the sequences of the conserved PCR fragments. The 5′ and 3′ RACE products were cloned and sequenced. The full-length cDNA of *sc*HIF-1α (MH709378) was 2848 bp, including a 5′-untranslated region (UTR) of 275 bp, a 3′-terminal UTR of 287 bp, and a 2286 bp open reading frame (ORF) encoding a protein of 762 amino acids (Fig. 1A). BLAST

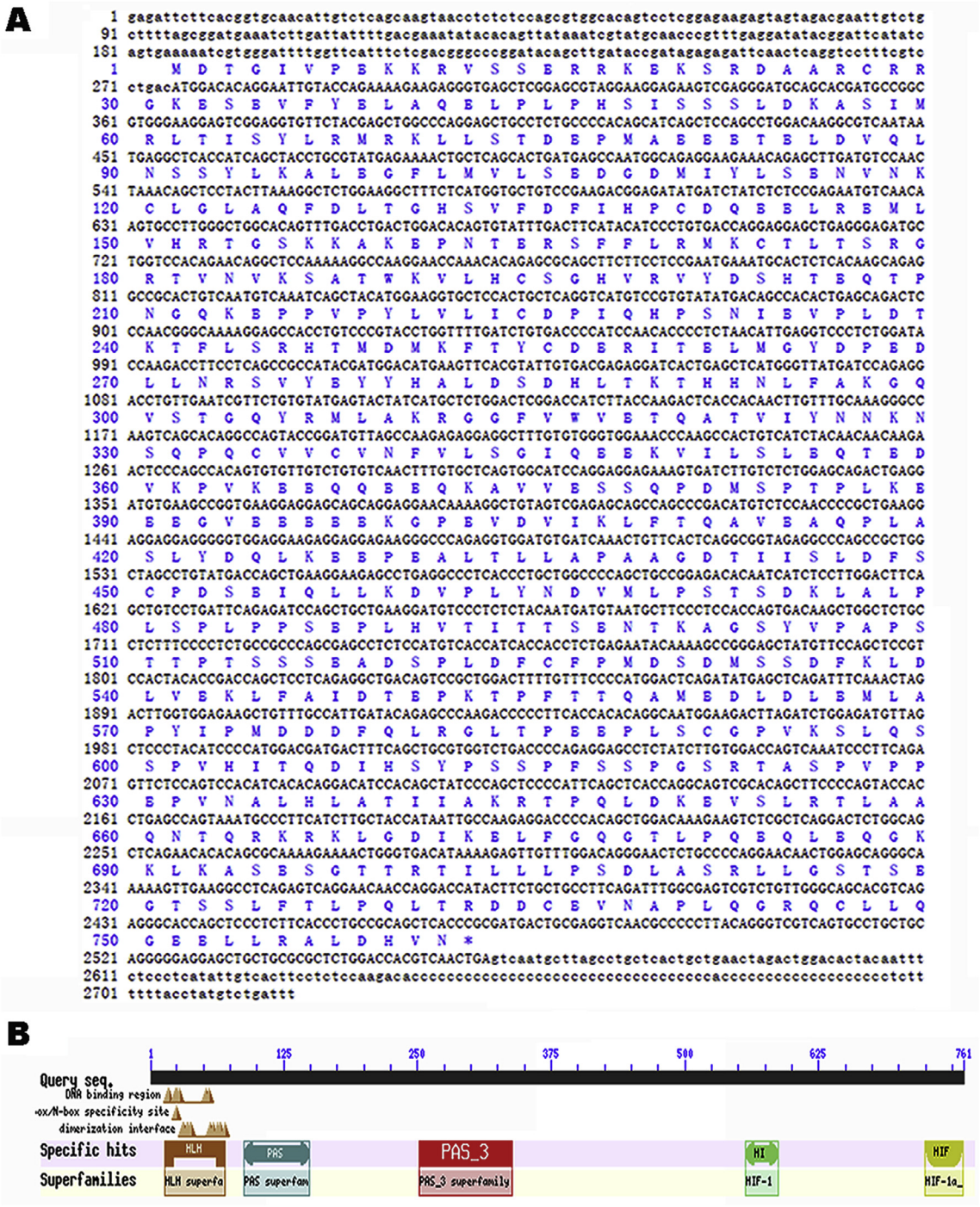

Fig. 1. Molecular cloning of mandarin fish *sc*HIF-1α. (A) Nucleotide sequence and the deduced amino acid sequence of *sc*HIF-1α. The entire deduced amino acid sequence is depicted using single letter codes beneath the corresponding nucleotide sequence. The stop codon is indicated by an asterisk. (B) Domain organization of *sc*HIF-1α. HLH indicates the helix-loop-helix domain, PAS indicates the PAS domain, PAS_3 indicates the PAS fold domain, HI indicates the DNA-binding domain, and HIF indicates the HIF-1α C-terminal transactivation domain.

homology analysis showed that the deduced amino acid sequences of *sc*HIF-1α matched well with HIF-1α from other species. SMART program analysis results indicated that *sc*HIF-1α contained five typical motifs: a helix-loop-helix domain, a PAS domain, a PAS fold, a DNA-binding domain, and a HIF-1α C-terminal transactivation domain (Fig. 1B). Considering that HIF-1α is a core protein of the HIF signaling pathway, our results suggested that the HIF signaling pathway was present in mandarin fish.

3.2. Multiple amino acid alignments and phylogenetic analysis

To study the evolutionary relationship of *sc*HIF-1α with other known proteins, multiple sequence alignments were performed using ClustalW 1.83 software. *sc*HIF-1α was highly homologous with other vertebrate HIF-1α proteins, shared similar architecture to vertebrate HIF-1α proteins, and contained similar action sites, such as hydroxylation on proline residue 402 and/or 564 and hydroxylation on asparagine residue 803 (Fig. 2A). The phylogenetic tree results revealed that the HIF-1α proteins were clustered into two major groups, namely,

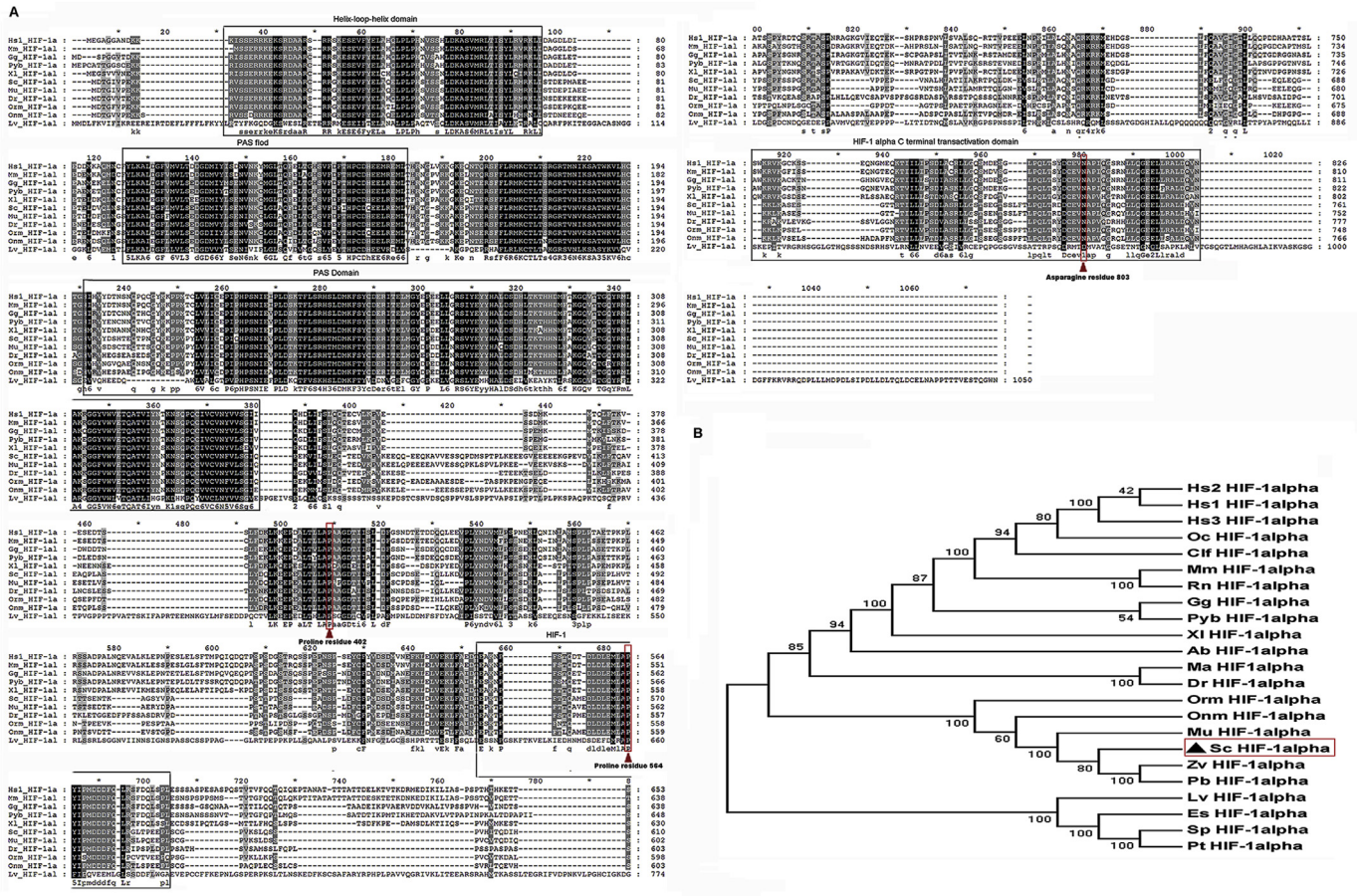

Fig. 2. Multiple sequence alignment and phylogenetic tree of the HIF-1α proteins from various species. (A) Multiple sequence alignment of the deduced amino acid sequences of HIF-1α proteins from 11 typical organisms. Numbers on the right indicate the amino acid positions. Identical (*) and similar (·or) residues are indicated below the alignment. (B) Phylogenetic tree of the HIF-1α proteins from various species. The phylogenetic tree was constructed according to the alignment of amino acid sequences using the neighbor-joining method in MEGA 5.0 and 1000 bootstrap replications. The bootstrap values are indicated at the nodes of the tree. The GenBank accession numbers of each HIF-1α are listed on the right side of the species name. Homo sapiens 1 (Hs1, NP_001521), Mus musculus (Mm, CAA64833), Gallus (Gg, NP_989628), Python bivittatus (Pyb, XM_007427209), Xenopus laevis (Xl, NM_001086980), Micropogonias undulatus (Mu, ABD32158), Danio rerio (Dr, NP_001296971), Oryzias melastigma (Orm, DQ317443), Oncorhynchus mykiss (Onm, NM_001124288), Litopenaeus vannamei (Lv, ACU30154). Homo sapiens 2 (Hs2, NP_851397), Homo sapiens 3 (Hs3, NP_001230013), Oryctolagus cuniculus (Oc, NP_001076251), Canis lupus familiaris (Clf, NP_001274092 XP_003639249), Rattus norvegicus (Rn, NP_077335), Acipenser baerii (Ab, ATY75506), Megalobrama amblycephala (Ma, ADF50043) Zoarces viviparus (Zv, AAZ52832), Python bivittatus (XM_007427209), Eriocheir sinensis (Es, AHH85804), Strongylocentrotus purpuratus (Sp, ASL69981), and Portunus trituberculatus (Pt, AQV08210).

vertebrate and invertebrate HIF-1α. Within the vertebrate HIF-1α cluster, *sc*HIF-1α formed a cluster with Pericformes HIF-1α, and this result was supported by a high bootstrap value. Thus, a close relationship was demonstrated between *sc*HIF-1α and other Pericformes HIF-1α (Fig. 2B).

3.3. Subcellular localization of scHIF-1α in MFF-1 cells

Subcellular localization is a dominant functional characteristic that is closely related to function. Immunofluorescence assay was used to determine the localization of *sc*HIF-1α in MFF-1 cells. The red fluorescence in Fig. 3 represents the Myc-tagged *sc*HIF-1α, which aggregated in the nucleus of MFF-1 cells. These observations suggested that overexpressed *sc*HIF-1α was mainly located in the nucleus in MFF-1 cells.

3.4. scHIF signaling pathway was induced by hypoxic stress

Dimethyloxallyl glycine (DMOG) is an inhibitor of HIF prolyl hydroxylase and is often used as an activator for the HIF signaling pathways [23]. The pGL4-HREs-luc plasmid contains HREs, which can be combined with HIF-1α. To investigate the HIF signaling pathway in mandarin fish, dual luciferase reporter assays were used. The pGL4-HREs-luc and pRT-TK were transiently co-transfected into MFF-1 cells. At 4 h post-transfection, cells were treated with DMOG. After 24 h of treatment, the firefly luciferase was detected, and *Renilla* luciferases were detected as the control. Compared with the control group, the relative expression level of luciferin increased by fourfold after the cells were treated with DMOG (Fig. 4A), thereby suggesting that the HIF signaling pathway was induced by DMOG in MFF-1 cells. To further verify these observations, the relative expression levels of the *sc*HIF signaling pathway downstream genes (*scglut-1*, *scvegf*, and *scldha*) were detected by qRT-PCR after the cells were treated with DMOG. Compared with those of the control groups, the relative expression levels of the *scldha*, *scvegf*, and *scglut-1* genes were significantly enhanced by 4.8, 5.2, and 21.3 times, respectively, after the cells were treated with DMOG (Fig. 4C). Furthermore, the mechanism by which the *sc*HIF signaling pathway could be induced by hypoxic stress (1% oxygen content, 1% O_2) was investigated in MFF-1 cells. Cells were cultured in the hypoxic culture system under 1% O_2. As a control, cells were cultured in a normoxic state (21% O_2). The luciferase reporter assay results showed that the relative expression level of luciferin increased by 40-fold in the hypoxia group compared with those of the normoxic control groups (Fig. 4B). Moreover, the relative expression levels of the *scglut-1*, *scvegf*, and *scldha* genes were significantly enhanced by 3.6, 3.1, and 6.9

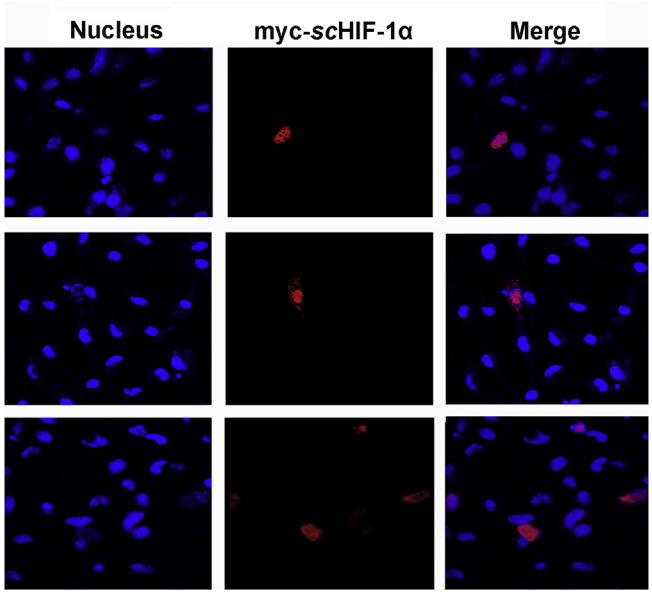

Fig. 3. Subcellular localization of *sc*HIF-1α in MFF-1 cells. MFF-1 cells were transfected with pCMV-Myc-*sc*HIF-1α plasmid. After allowing the cells to adhere for 48 h in 24-well plates, the nucleus was stained with Hoechst 33342, and fluorescent signals were observed under a fluorescence microscope (Magnification: ×630).

times in the hypoxia group, respectively, compared with those of the normoxic control groups (Fig. 4D). Therefore, the *sc*HIF signaling pathway was induced by hypoxic stress in MFF-1 cells.

3.5. The HIF signaling pathway was regulated by scHIF-1α

To investigate the role of *sc*HIF-1α in the HIF signaling pathway, dual luciferase reporter assays were used to detect the activity of HRE-luc after the cells were transfected with pGL4-HREs-luc, pCMV-myc-*sc*HIF-1α and pRL-TK plasmids. The relative level of luciferin was doubled after the overexpression of *sc*HIF-1α (Fig. 5A). Using qRT-PCR, the relative expression levels of the *scldha*, *scvegf*, and *scglut-1* genes were detected and found to be significantly enhanced after the cells were transfected with the pCMV-myc-*sc*HIF-1α compared with those of cells transfected with the pCMV-myc plasmid (as a control) (Fig. 5C). These results suggested that the *sc*HIF signaling pathway was obviously induced by *sc*HIF-1α in MFF-1 cells.

RNAi is widely used to determine the function of genes. To detect the efficiency of si-*sc*HIF-1α, si-*sc*HIF-1α with different concentrations (20, 50, and 100 nM) and pCMV-myc-*sc*HIF-1α were co-transfected into MFF-1 cells, and the expression levels of *sc*HIF-1α was detected by Western blot or qRT-PCR. The mRNA and protein levels of *sc*HIF-1α were significantly reduced after the cells were transfected with 100 nM si-*sc*HIF-1α compared with those of cells that were transfected with control siRNA (si-NC) (Fig. 5B). Thus, cells transfected with 100 nM si-*sc*HIF-1α could down-regulate the *sc*HIF-1α levels. To further confirm the role of *sc*HIF-1α in the HIF signaling pathway, the expression levels of the *scldha*, *scvegf*, and *scglut-1* genes were detected after the cells were transfected with si-*sc*HIF-1α and then stimulated by DMOG (Fig. 5D). The expression levels of the *scldha*, *scvegf*, and *scglut-1* genes in the DMOG groups were significantly higher than those in the control groups. In the DMOG groups, the expression levels of the *scldha*, *scvegf*, and *scglut-1* genes after the cells were transfected with si-*sc*HIF-1α were significantly lower than those of cells transfected with si-NC. The expression levels of the *scldha*, *scvegf*, and *scglut-1* genes were also detected after the cells were transfected with si-*sc*HIF-1α under hypoxic stress (Fig. 5E). As expected, the expression levels of the *scldha*, *scvegf*, and *scglut-1* genes in the hypoxia groups (1% O_2) were significantly higher than those in the normoxic control groups (21% O_2). In the hypoxia group (1% O_2), the expression levels of the *scldha*, *scvegf*, and *scglut-1* genes after the cells were transfected with si-*sc*HIF-1α were also significantly lower than those of cells transfected with si-NC. These

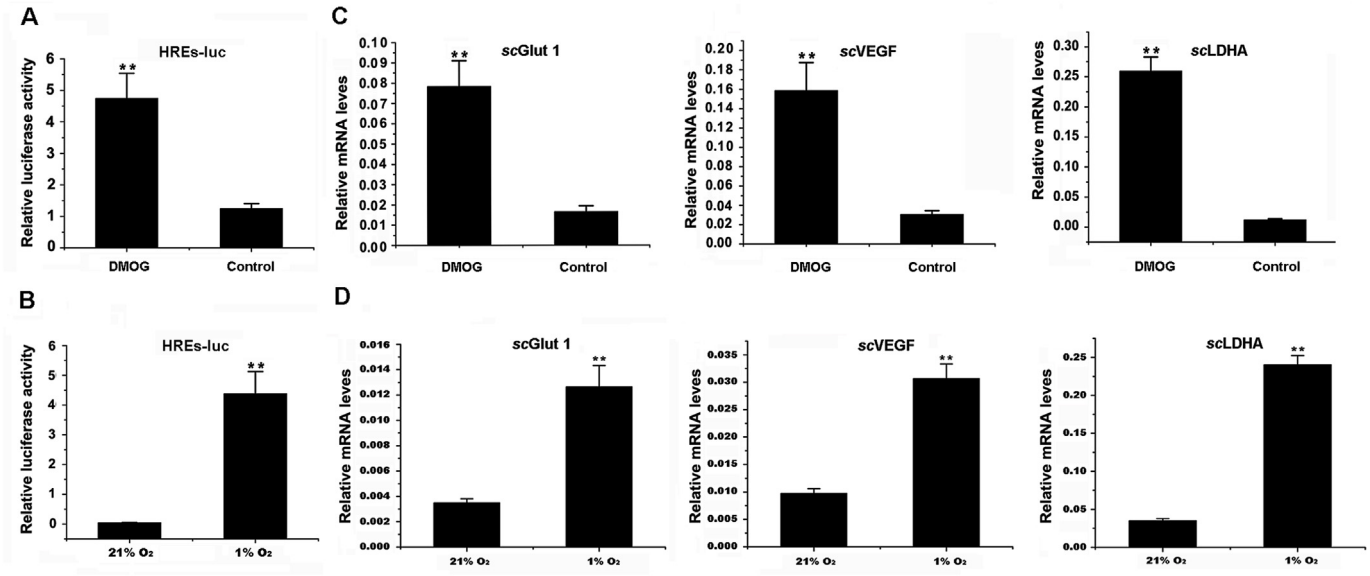

Fig. 4. The *sc*HIF signaling pathway was activated by DMOG or hypoxic stress in MFF-1 cells. In (A) and (B), MFF-1 cells were seeded on 24-well plates overnight and co-transfected with plasmids pGL4-HREs-luc and pRT-TK. At 4 h post-transfection, cells were treated with DMOG (1 mM) or hypoxic stress (1% O_2). For the control, cells were mock treated or cultured in a normoxic state (21% O_2). The luciferase activities were measured at 24 h post-transfection. The luciferase activity value was achieved against the *Renilla* luciferase activity. The *y*-axis represents the relative luciferase activities. Data are presented as the means ± SE from three independent triplicated experiments. **, $p < 0.01$ and *, $p < 0.05$ versus the controls. In (C) and (D), the relative expression levels of the *scglut-1*, *scvegf*, and *scldha* genes were detected after cells were treated with DMOG (1 mM) or hypoxic stress (1% O_2). Total RNAs were extracted, and *β-actin* served as an internal control to calibrate the cDNA template for all samples. The *y*-axis represents the relative mRNA expression. Line points indicate the mean ± SD of five technical replicates. Statistical analysis of the differences was performed by one-way ANOVA using SPSS v20.0 software. The asterisks above the bars represent statistically significant differences of the control samples. "*" at $p < 0.05$ and "**" at $p < 0.01$.

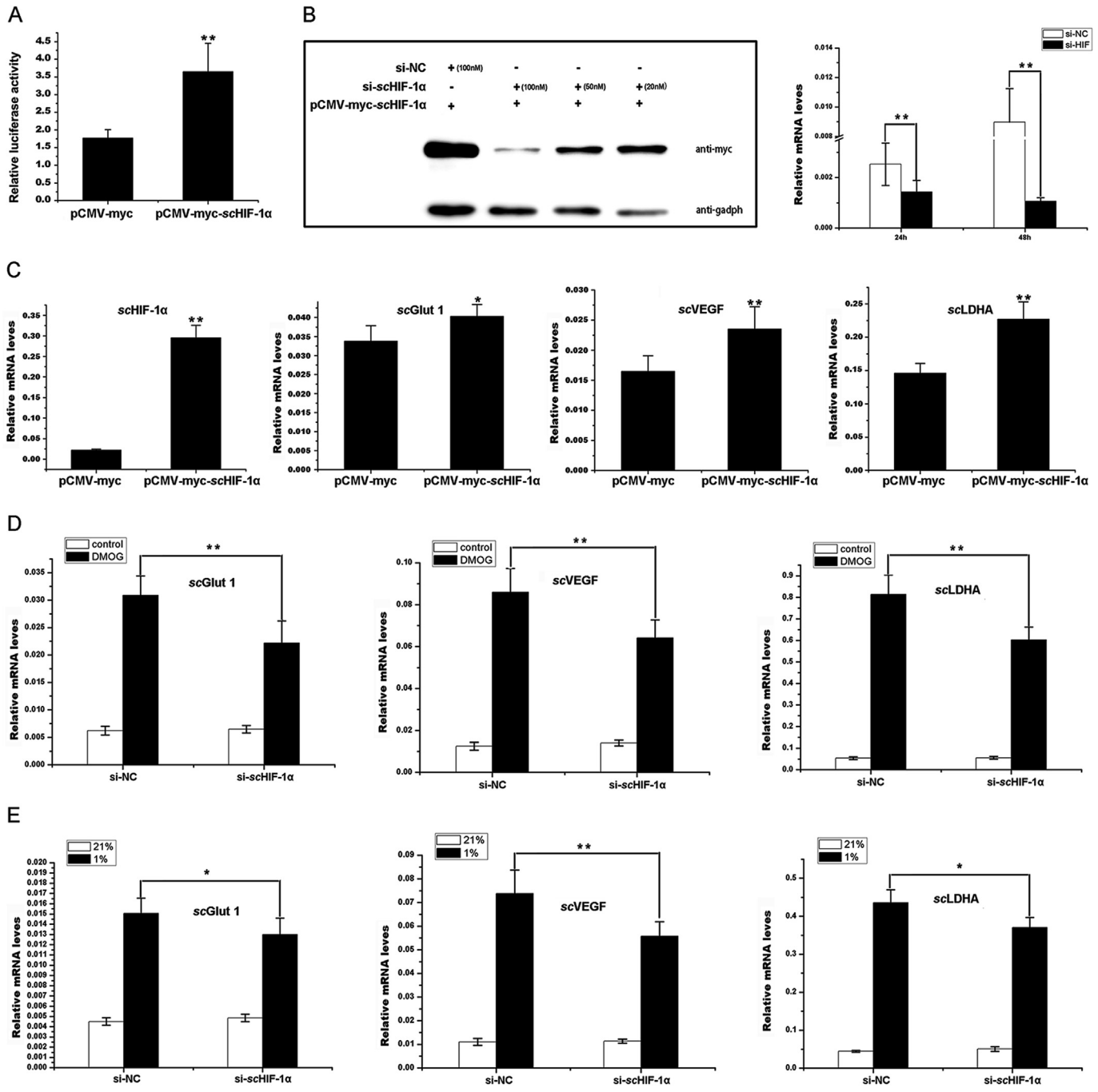

Fig. 5. HIF signaling pathway was regulated by *sc*HIF-1α in MFF-1 cells. (A) The *sc*HIF signaling pathway was stimulated by *sc*HIF-1α overexpression in MFF-1 cells. The plasmids of pGL4-HREs-luc, pCMV-myc-*sc*HIF-1α, and pRL-TK were co-transfected into MFF-1 cells. The luciferase activity value was achieved against *Renilla* luciferase activity. The *y*-axis represents the relative luciferase activities. Data are presented as the mean ± SE from three independent triplicated experiments. **, $p < 0.01$; and *, $p < 0.05$ versus the controls. (B) The knockdown effect of si-*sc*HIF-1α. si-*sc*HIF-1α with different concentrations (20, 50, 100 nM) and pCMV-myc-*sc*HIF-1α were co-transfected into MFF-1 cells. The mRNA and protein levels of myc-*sc*HIF-1α were detected by qRT-PCR and Western blot at 24 h post-transfection. The expression patterns of the *schif-1α, scglut-1, scvegf*, and *scldha* genes were detected using qRT-PCR, following *schif-1α* overexpression of the cells (C), transfection of the cells with 100 nM si-*sc*HIF-1α, and treatment with DMOG (D) or under hypoxic stress (1% O_2) (E). For the controls, the cells were transfected with pCMV-Myc plasmid (C), mock treated (D), or cultured in a normoxic state (21% O_2) (E). Total RNAs were extracted, and *β-actin* served as an internal control to calibrate the cDNA template for all samples. The *y*-axis represents the relative mRNA expression. Line points indicate the mean ± SD of five technical replicates. Statistical analysis of differences was performed by one-way ANOVA using SPSS v20.0 software. The asterisks above the bars represent statistically significant differences of the control samples. "*" at $p < 0.05$ and "**" at $p < 0.01$.

results suggested that *sc*HIF-1α could regulate the HIF signaling pathway in mandarin fish.

3.6. Tissue distributions of scHIF-1α

Quantitative real-time PCR was performed to determine the expression levels of *schif-1α* in different tissues of mandarin fish, including the liver, gill, fat, brain, fin, spleen, heart, blood, intestine, hind kidney,

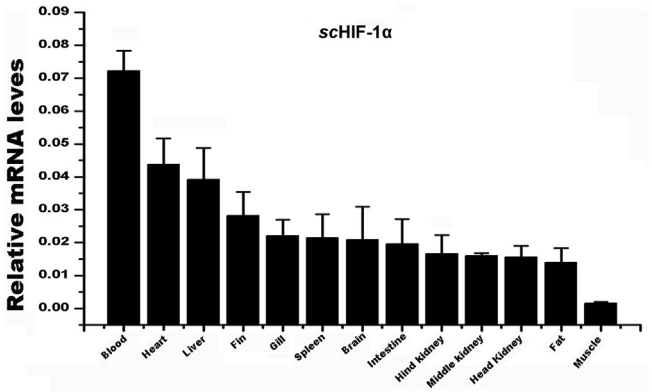

Fig. 6. Expression levels of the *schif-1α* gene in various mandarin fish tissues. Total RNAs were extracted from the liver, gill, fat, brain, fin, spleen, heart, blood, intestine, hind kidney, middle kidney, head kidney, and muscle. The *β-actin* gene served as an internal control to calibrate the cDNA template for all samples. The *y*-axis represents the relative mRNA expression. Each bar signifies the mean ± SEM of triplicate samples, and the data are representative of two independent experiments.

middle kidney, head kidney, and muscle. The *β-actin* gene was used as an internal control in all reactions. Results revealed that the *schif-1α* gene was widely expressed in all the tissues tested (Fig. 6). The levels of *schif-1α* transcripts were significantly highly expressed in the blood, heart, and liver than in the other tissues tested. These outcomes implied that the main physiological function of *sc*HIF-1α was closely related to the circulatory system and might be involved in oxygen metabolism and immune response.

3.7. Transcriptional regulation of scHIF-1α in response to immune challenge

To investigate whether *sc*HIF-1α expression is regulated by the immune challenge, qRT-PCR was performed to determine the expression levels of *schif-1α* after the MFF-1 cells were treated with poly I:C, poly dG:dC, and PMA. The expression levels of the *scmx, scifn-h, sctnf-α and scil-18* genes significantly increased, thereby indicating that the cells were stimulated by poly I:C (Fig. 7A), poly dG:dC (Fig. 7B), and PMA (Fig. 7C). The relative expression levels of the *schif-1α* gene were also significantly enhanced by 3.6-, 3.1-, and 6.9-fold after 24 h of treatment with poly I:C, poly dG:dC, and PMA, respectively. These results indicated that *sc*HIF-1α was involved in the innate immune response of mandarin fish.

3.8. scHIF-1α could inhibit MRV and SCRV infections in MFF-1 cells

The MRV and SCRV are two important and different types (DNA virus and RNA virus) of viral agents of mandarin fish. To investigate the potential role of *sc*HIF-1α in viral infection, the overexpression or knockdown of *sc*HIF-1α was used. MFF-1 cells were transfected with pCMV-myc-*sc*HIF-1α or si-*sc*HIF-1α, with the pCMV-myc empty plasmid or si-NC as the control. After transfection, the MRV- or SCRV-infected cells were employed to determine the expression levels of the major capsid protein (*mcp*) gene of the virus using qRT-PCR. The expression levels of the *mcp* gene decreased by 69.6- or 1.4-fold after the cells were transfected with pCMV-myc-*sc*HIF-1α and then infected with

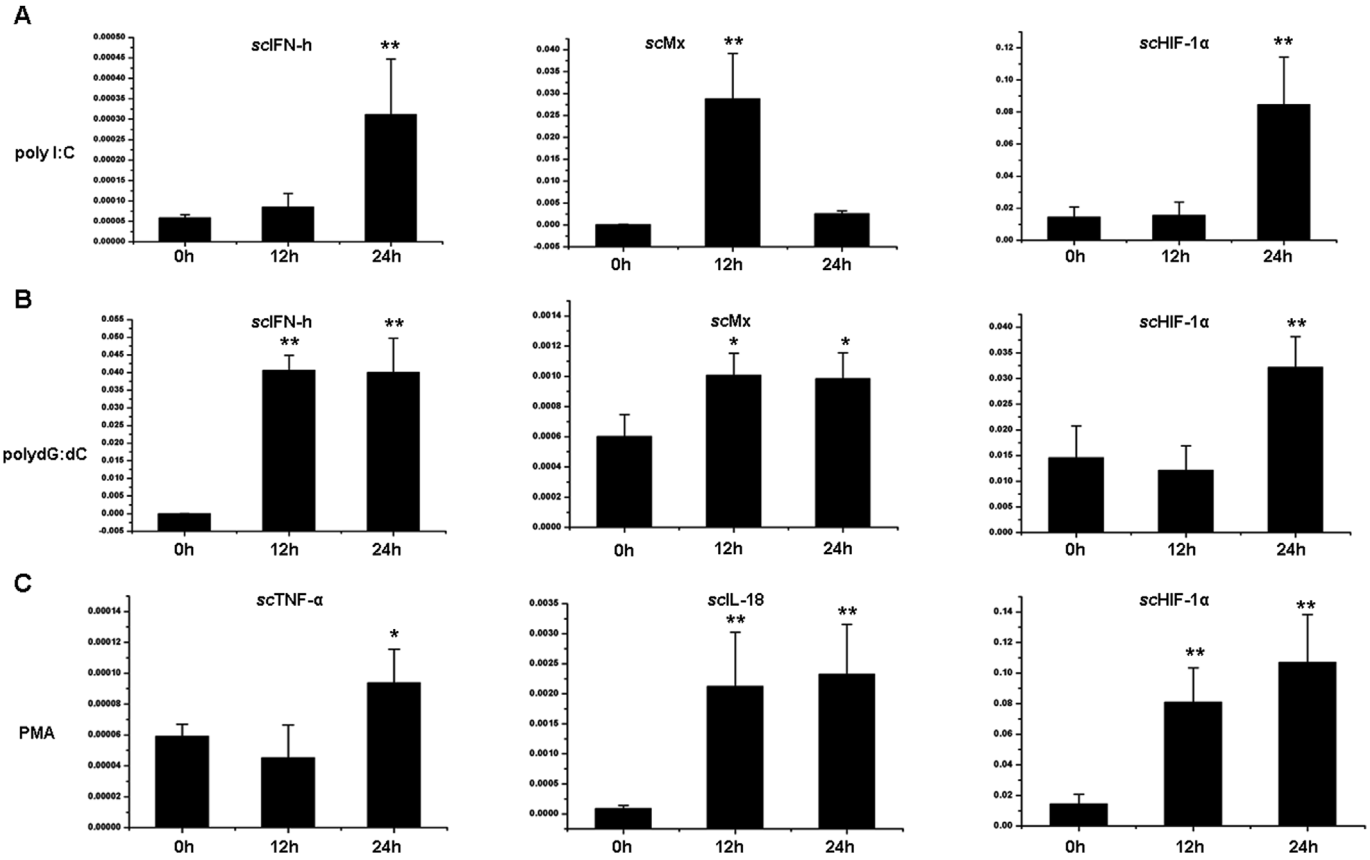

Fig. 7. *schif-1α* gene expression levels were regulated by the immune challenges. (A) Expression patterns of *schif-1α, scifn-h*, and *scmx* under stimulation by poly I:C. (B) Expression patterns of *schif-1α,scifn-h*, and *scmx* under stimulation by poly dG:dC. (C) Expression patterns of *schif-1α, sctnf-α*, and *scil-18* under stimulation by PMA. The *y*-axis represents the relative mRNA expression. Line points represent the mean ± SD of five technical replicates. Statistical analysis of the differences was performed by one-way ANOVA using SPSS v20.0 software. The asterisks above the bars represent statistically significant differences of the control samples. "*" at $p < 0.05$ and "**" at $p < 0.01$.

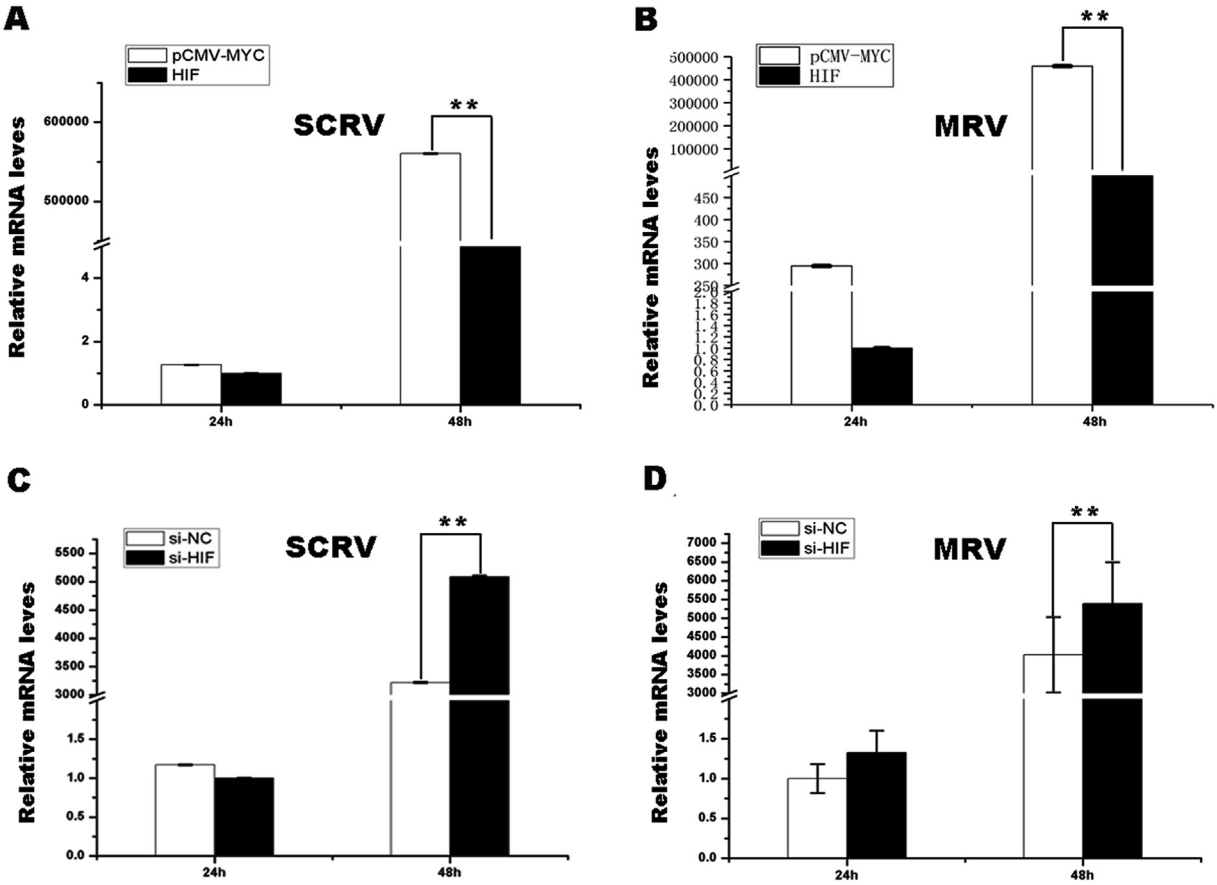

Fig. 8. MRV and SCRV infections were inhibited by *sc*HIF-1α in MFF-1 cells. The *mcp* mRNA levels of SCRV (A) and MRV (B) were detected by qRT-PCR after the cells overexpressed *sc*HIF-1α. Cells transfected with the pCMV-myc empty plasmid constituted the control. The *mcp* mRNA levels of SCRV (C) and MRV (D) were detected by qRT-PCR, after the cells were transfected with si-*sc*HIF-1α. Cells transfected with si-NC were used as the control. The *y*-axis represents the relative mRNA levels. Line points represent the mean ± SD of five technical replicates. Statistical analysis of the differences was performed by one-way ANOVA using SPSS v20.0 software. The asterisks above the bars represent statistically significant differences of the control samples. "*" at $p < 0.05$ and "**" at $p < 0.01$.

MRV or SCRV (Fig. 8A and B). The results of *sc*HIF-1α knockdown further verified the findings from its overexpression. When *sc*HIF-1α knockdown was implemented with si-RNA, the expression levels of the MRV or SCRV *mcp* genes increased by 1.34 or 1.58 times, respectively (Fig. 8C and D). These findings suggested that MRV and SCRV infections were inhibited by *sc*HIF-1α in the MFF-1 cells.

4. Discussion

Oxygen is an essential element for normal aerobic metabolism in animals [24,25]. Oxygen depletion is a universal phenomenon that occurs in aquatic environments. To deal with hypoxic stress, fishes have adapted and developed a series of regulatory mechanisms for living in hypoxic conditions [26]. The HIF signaling pathway is the main regulatory pathways under hypoxia, for which HIF-1α is a key protein. With increasing density of breeding, aquaculture is often performed under hypoxia [8]. Investigating the hypoxic stress signaling pathways in farmed fish is urgently needed. Our results showed that the characteristic of mandarin fish *sc*HIF-1α was similar to that of mammalian HIF-1α, and the former could regulate the *sc*HIF signaling pathway. Furthermore, *sc*HIF-1α was involved in the fish immune response. Overexpression of *sc*HIF-1α could inhibit the tested viral infections, and knockdown of *sc*HIF-1α could promote the tested viral infections. The above observations suggested that *sc*HIF-1α plays an important role in fish hypoxic stress and is involved in fish viral infection.

The HIF signaling pathway is ancient and conservative and is present in the earliest stages of animal oxygen-sensing evolution from fish to humans [27]. In this study, the *sc*HIF signaling pathway was induced by hypoxic stress in the investigated MFF-1 cells. The *sc*HIF signaling pathway was activated after being induced by DMOG or hypoxic stress (1% O_2) in MFF-1 cells as verified by the luciferase reporter assays and qRT-PCR. This result indicated that mandarin fish also had a HIF signaling pathway to adapt to hypoxic stress. The sequence characteristics and the architecture of the *sc*HIF-1α protein was similar to those of other vertebrate HIF-1α proteins (Fig. 1). Transiently overexpressing *sc*HIF-1α could induce the HIF signaling pathway, and knockdown of *sc*HIF-1α could inhibit the HIF signaling pathway (Fig. 6). Therefore, *sc*HIF-1α acted as a transcriptional regulator and was also similar to the other species of HIF-1α proteins. Furthermore, proline residues 402 and 564 were the most important regulatory sites of HIF-1α. prolyl hydroxylase domain proteins can recognize and hydroxylate these two proline residues, thereby leading to proteasomal degradation [28]. The asparagine residue 803 is another important regulatory site of HIF-1α and may be hydroxylated by FIH (factor-inhibiting hypoxia-inducible factor 1) [29]. Hydroxylation of this aspartic acid residue in HIF-1α can inhibit HIF-1α activity [29]. Unsurprisingly, the proline residues 402 and 564 and asparagine residue 803 were also present in *sc*HIF-1α (Fig. 2A). Accordingly, we speculated that mandarin fish might share a similar mechanism of negative HIF-1 regulation to other vertebrates. The above results suggested that HIF-1α and its induced hypoxia signaling pathway were highly conserved from fish to mammals.

The HIF signaling pathway not only plays an integral role in driving cellular adaptation to low oxygen but also interacts with the immune responses [30]. Such a pathway can both regulate many immune-related genes and respond to the immune system [31]. In this study, the involvement of *sc*HIF-1α in the immune response and the inhibition of

fish viral infections were discussed. The expression levels of *sc*HIF-1α significantly increased after the cells were treated with poly I:C, poly dG:dC, and PMA. Those results indicated that *sc*HIF-1α could respond to immunity stimulation, and the mandarin fish HIF signaling pathway participated in immunity.

HIF-1α also plays important roles in pathogenic infections in mammals [4], but related investigations in fish remain scarce. The involvement of *sc*HIF-1α in viral infection was investigated. Overexpression of *sc*HIF-1α could inhibit MRV and SCRV infections. The corresponding opposite results revealed that knockdown of the *sc*HIF-1α could promote MRV and SCRV infections. Those observations suggested that *sc*HIF-1α participated in fish viral infections. The connection between HIF-1α and viral infection is an interesting topic. On the one hand, the virus can hijack the HIF-1α for its benefit. For instance, the HIF-1α transcripts increased in the gills, hepatopancreas, and muscle after WSSV infection, and this occurrence may help WSSV replication by reprogramming the host metabolism (The Warburg effect) [32,33]. Moreover, the knockout of the HIF-1α gene in *epithelioma papulosum cyprini* cells inhibited apoptosis and the growth of the viral hemorrhagic septicemia virus [34]. On the other hand, HIF-1α can activate the HIF signaling pathway to inhibit the virus [35]. The replication of vesicular stomatitis virus is inhibited by hypoxia-induced HIF [19], and the constitutive expression of HIF-1α appears to restrict H-1 viral replication [36]. Our study demonstrated that *sc*HIF-1α inhibited MRV and SCRV infections, but the details of the mechanism involved require further study.

Acknowledgement

This work was supported by the National Key Research and Development Program of China (Nos.2018YFD0900504 and 2018YFD0900501), the National Natural Science Foundation of China (No. 31702381), the Guangdong Natural Science Foundation (Nos. 2016B020202001 and 2014TQ01N303), the Science and Technology Planning Project of Guangzhou (Nos. 201805300104 and 201607020014), the China Agricultural Research System (No. CARS-46), and the Guangdong Key Research and Development Program (No. 2019B020217001).

Appendix A. Supplementary data

Supplementary data to this article can be found online at https://doi.org/10.1016/j.fsi.2019.04.298.

References

[1] K.A. Nolan, C.C. Scholz, Hypoxia: from basic mechanisms to therapeutics - a meeting report on the Keystone and HypoxiaNet Symposium, Hypoxia (Auckl) 3 (2015) 67–72.
[2] M. Kappler, H. Taubert, A.W. Eckert, Oxygen sensing, homeostasis, and disease, N. Engl. J. Med. 365 (2011) 1845–1846 1846.
[3] K.A. Webster, Evolution of the coordinate regulation of glycolytic enzyme genes by hypoxia, J. Exp. Biol. 206 (2003) 2911–2922.
[4] A. Palazon, A.W. Goldrath, V. Nizet, R.S. Johnson, HIF transcription factors, inflammation, and immunity, Immunity 41 (2014) 518–528.
[5] R.K. Bruick, S.L. McKnight, A conserved family of prolyl-4-hydroxylases that modify HIF, Science 294 (2001) 1337–1340.
[6] T. Kamura, S. Sato, K. Iwai, M. Czyzyk-Krzeska, R.C. Conaway, J.W. Conaway, Activation of HIF1alpha ubiquitination by a reconstituted von Hippel-Lindau (VHL) tumor suppressor complex, Proc. Natl. Acad. Sci. U. S. A. 97 (2000) 10430–10435.
[7] M.C. Simon, L. Liu, B.C. Barnhart, R.M. Young, Hypoxia-induced signaling in the cardiovascular system, Annu. Rev. Physiol. 70 (2008) 51–71.
[8] W. Xiao, The hypoxia signaling pathway and hypoxic adaptation in fishes, Sci. China Life Sci. 58 (2015) 148–155.
[9] A.J. Harris, A.R. Thompson, M.K. Whyte, S.R. Walmsley, HIF-mediated innate immune responses: cell signaling and therapeutic implications, Hypoxia (Auckl) 2 (2014) 47–58.
[10] H.K. Bayele, C. Peyssonnaux, A. Giatromanolaki, W.W. Arrais-Silva, H.S. Mohamed, H. Collins, et al., HIF-1 regulates heritable variation and allele expression phenotypes of the macrophage immune response gene SLC11A1 from a Z-DNA forming microsatellite, Blood 110 (2007) 3039–3048.
[11] S. Lin, S. Wan, L. Sun, J. Hu, D. Fang, R. Zhao, et al., Chemokine C-C motif receptor 5 and C-C motif ligand 5 promote cancer cell migration under hypoxia, Cancer Sci. 103 (2012) 904–912.
[12] R. Du, K.V. Lu, C. Petritsch, P. Liu, R. Ganss, E. Passegue, et al., HIF1alpha induces the recruitment of bone marrow-derived vascular modulatory cells to regulate tumor angiogenesis and invasion, Cancer Cell 13 (2008) 206–220.
[13] J. Rius, M. Guma, C. Schachtrup, K. Akassoglou, A.S. Zinkernagel, V. Nizet, et al., NF-kappaB links innate immunity to the hypoxic response through transcriptional regulation of HIF-1alpha, Nature 453 (2008) 807–811.
[14] E.V. Dang, J. Barbi, H.Y. Yang, D. Jinasena, H. Yu, Y. Zheng, et al., Control of T(H)17/T(reg) balance by hypoxia-inducible factor 1, Cell 146 (2011) 772–784.
[15] A. Ikejiri, S. Nagai, N. Goda, Y. Kurebayashi, M. Osada-Oka, K. Takubo, et al., Dynamic regulation of Th17 differentiation by oxygen concentrations, Int. Immunol. 24 (2012) 137–146.
[16] H. Nakamura, Y. Makino, K. Okamoto, L. Poellinger, K. Ohnuma, C. Morimoto, et al., TCR engagement increases hypoxia-inducible factor-1 alpha protein synthesis via rapamycin-sensitive pathway under hypoxic conditions in human peripheral T cells, J. Immunol. 174 (2005) 7592–7599.
[17] J.E. Albina, B. Mastrofrancesco, J.A. Vessella, C.A. Louis, W.J. Henry, J.S. Reichner, HIF-1 expression in healing wounds: HIF-1alpha induction in primary inflammatory cells by TNF-alpha, Am. J. Physiol. Cell Physiol. 281 (2001) C1971–C1977.
[18] N. Vassilaki, E. Frakolaki, Virus-host interactions under hypoxia, Microb. Infect. 19 (2017) 193–203.
[19] Hwang II, I.R. Watson, S.D. Der, M. Ohh, Loss of VHL confers hypoxia-inducible factor (HIF)-dependent resistance to vesicular stomatitis virus: role of HIF in antiviral response, J. Virol. 80 (2006) 10712–10723.
[20] S. Pina-Oviedo, K. Khalili, V.L. Del, Hypoxia inducible factor-1 alpha activation of the JCV promoter: role in the pathogenesis of progressive multifocal leukoencephalopathy, Acta Neuropathol. 118 (2009) 235–247.
[21] S.L. Deshmane, S. Amini, S. Sen, K. Khalili, B.E. Sawaya, Regulation of the HIV-1 promoter by HIF-1alpha and Vpr proteins, Virol. J. 8 (2011) 477.
[22] C. Dong, S. Weng, X. Shi, X. Xu, N. Shi, J. He, Development of a Mandarin fish Siniperca chuatsi fry cell line suitable for the study of infectious spleen and kidney necrosis virus (ISKNV), Virus Res. 135 (2008) 273–281.
[23] X. Li, H. Zhao, Y. Wu, S. Zhang, X. Zhao, Y. Zhang, et al., Up-regulation of hypoxia-inducible factor-1alpha enhanced the cardioprotective effects of ischemic post-conditioning in hyperlipidemic rats, Acta Biochim. Biophys. Sin. 46 (2014) 112–118.
[24] B. Ekblom, A.N. Goldbarg, A. Kilbom, P.O. Astrand, Effects of atropine and propranolol on the oxygen transport system during exercise in man, Scand. J. Clin. Lab. Invest. 30 (1972) 35–42.
[25] Y. Bouffard, J.P. Viale, G. Annat, C. Guillaume, C. Percival, O. Bertrand, et al., Pulmonary gas exchange during hemodialysis, Kidney Int. 30 (1986) 920–923.
[26] P.E. Bickler, L.T. Buck, Hypoxia tolerance in reptiles, amphibians, and fishes: life with variable oxygen availability, Annu. Rev. Physiol. 69 (2007) 145–170.
[27] Y. Okamura, T. Mekata, G.E. Elshopakey, T. Itami, Molecular characterization and gene expression analysis of hypoxia-inducible factor and its inhibitory factors in kuruma shrimp Marsupenaeus japonicus, Fish Shellfish Immunol. 79 (2018) 168–174.
[28] A.C. Epstein, J.M. Gleadle, L.A. McNeill, K.S. Hewitson, J. O'Rourke, D.R. Mole, et al., C. elegans EGL-9 and mammalian homologs define a family of dioxygenases that regulate HIF by prolyl hydroxylation, Cell 107 (2001) 43–54.
[29] K.S. Hewitson, L.A. McNeill, M.V. Riordan, Y.M. Tian, A.N. Bullock, R.W. Welford, et al., Hypoxia-inducible factor (HIF) asparagine hydroxylase is identical to factor inhibiting HIF (FIH) and is related to the cupin structural family, J. Biol. Chem. 277 (2002) 26351–26355.
[30] E. Krzywinska, C. Stockmann, Hypoxia, metabolism and immune cell function, Biomedicines 6 (2018).
[31] E.P. Cummins, C.E. Keogh, D. Crean, C.T. Taylor, The role of HIF in immunity and inflammation, Mol. Asp. Med. 47–48 (2016) 24–34.
[32] M. Hernandez-Palomares, J.A. Godoy-Lugo, S. Gomez-Jimenez, L.A. Gamez-Alejo, R.M. Ortiz, J.F. Munoz-Valle, et al., Regulation of lactate dehydrogenase in response to WSSV infection in the shrimp Litopenaeus vannamei, Fish Shellfish Immunol. 74 (2018) 401–409.
[33] M.M. Miranda-Cruz, J.J. Poom-Llamas, J.A. Godoy-Lugo, R.M. Ortiz, S. Gomez-Jimenez, J.A. Rosas-Rodriguez, et al., Silencing of HIF-1 in WSSV-infected white shrimp: effect on viral load and antioxidant enzymes, Comp. Biochem. Physiol. C Toxicol. Pharmacol. 213 (2018) 19–26.
[34] M.S. Kim, K.H. Kim, CRISPR/Cas9-mediated knockout of HIF-1alpha gene in epithelioma papulosum cyprini (EPC) cells inhibited apoptosis and viral hemorrhagic septicemia virus (VHSV) growth, Arch. Virol. 163 (2018) 3395–3402.
[35] F. Morinet, M. Parent, C. Bergeron, S. Pillet, C. Capron, Oxygen and viruses: a breathing story, J. Gen. Virol. 96 (2015) 1979–1982.
[36] I.R. Cho, S. Kaowinn, J. Moon, J. Soh, H.Y. Kang, C.R. Jung, et al., Oncotropic H-1 parvovirus infection degrades HIF-1alpha protein in human pancreatic cancer cells independently of VHL and RACK1, Int. J. Oncol. 46 (2015) 2076–2082.